JETIR.ORG ISSN: 2349-5162 | ESTD Year : 2014 | Monthly Issue
JOURNAL OF EMERGING TECHNOLOGIES AND INNOVATIVE RESEARCH (JETIR)
An International Scholarly Open Access, Peer-reviewed, Refereed Journal

Knootwood-Mediated Synthesis of Zinc Oxide Nanoparticles: Influence of Extract Volume on Crystallinity, Morphology, and Antifungal Efficiency

Gaurav Pandey[1*], Vinay Kumar Varshney[1]
[1]Forest Research Institute (FRI), Dehradun, Uttarakhand – 248006 (India)

Abstract

In the present work, we discuss an eco-friendly and low-cost approach for the synthesis of ZnO nanoparticles with different concentrations of Knootwood (knootwood) extract. The formed nanoparticles were characterized by FT-IR, XRD and TEM. These ZnO particles showed a unique Zn-O bond at 618 cm^{-1} and a pure hexagonal Wurtzite phase. The shape and size of the particles could be influenced by load of the knootwood extract, and the uniformity of particles was related with it. The antifungal performance of the prepared ZnO nanoparticles was determined by decomposing methylene blue in the presence of UV light. The biosynthesized nanoparticles were found to exhibit far greater degradation rates when compared to commercially available ZnO particles.

Keywords: Zinc Oxide Nanoparticles, Green Synthesis, knotwood Extract, Nanoparticle Morphology, Antifungal efficacy

1. Introduction

Increases in the emission of toxic dyes into waste water have led to a greater need for improved and environmentally friendly waste water treatment technologies [1, 2]. Out of the various techniques such as adsorption, flocculation, ozonation, and antifungal antifungal is more popular due to its simplicity, nontoxic nature, stability, effectiveness in the decomposition of complex dye molecules [3, 4].

Zinc oxide (ZnO), a semiconductor with a room temperature band gap of 3.37 eV, has been extensively investigated as a photocatalyst [1–8]. Due to its low price, high photo-reactivity, and environmental compliance, it is an attractive candidate for a such application [5]. ZnO is a nanoscale material, and the structured ZnO has the advantage of a large specific surface area, high Fermi level and good catalytic ability, so its antifungal performance is much higher than that of bulk ZnO [6, 7].

Various methods have been utilized for the preparation of ZnO nanoparticles, such as CVD method, gas phase synthesis, spray pyrolysis, hydrothermal, electrochemical, microwave assisted synthesis, and sol-gel process [8]. However, these methods are usually assisted by toxic chemicals and the residual toxicity coated on the surface of the nanoparticle restrict their applications in biomedicine.

Green synthesis procedures and in particular those using biological species such as plants and microorganisms represent a greener approach. These methods, besides being economical, eliminate the environmental load of toxic reagents [9–11]. For example, Shankar et al have shown the generation of gold and silver nanoparticles using Azadirachta indica (Neem) leaf broth instead of hazardous chemical as reducing agent [12].

Medicinal plant extracts involved in green synthesis serve as reducing and stabilizing agents. They have the capability of mass production of nanoparticles with significantly low environmental pollution [13–15]. Among these plants, Knootwood has been considered as a potential source due to its abundant content of bioactive phenolic and terpenoid molecules. These biomolecules are known to possess antimicrobial, antioxidant activities and to help in the reduction of metal ions in addition of stabilizing the synthesized nanoparticles [16, 17].

The ability of knootwood extract to assist the synthesis of Nanoparticles has been explained in terms of the polyphenolic groups of knootwood extract interacting with the metal ions. Especially, aromatic hydroxyl groups can make stable complexes with zinc ions, which would be thermally decomposed to produce ZnO nanoparticles [18,19]. Although antibacterial activity of ZnO synthesized by knootwood extract has been previously reported [20, 21], how concentration of Knootwood extract affects characteristics of the ZnO nanoparticles has not been systematically studied.

The present study aims to fill this gap and describes green synthesis of Wurtzite-phase ZnO NPs, with varying volumes of knootwood extract. Their antifungal behavior for the degradation of methylene blue under UV irradiation is also investigated.

2. Materials and Methods

2.1 Materials

Knot wood biomass Neem (Azadirachta indica) was collected from the Range Office, Forest Research Institute (FRI), Dehradun, in January 2020. Experiments were conducted using Milli-Q water, and all required chemicals, including zinc acetate dihydrate [$Zn(CH_3COO)_2 . 2H_2O$], were procured from Sigma-Aldrich, India.

2.2 Preparation of the Plant Extract

Freshly dried Azadirachta indica biomass was chopped, lyophilized for 72 hours, powdered, and extracted using 25% aqueous methanol to isolate bioactive phenolics. Ultrasonication aided extraction, followed by concentration at 40°C using a rotary evaporator. The extract was vacuum-sealed and stored at 4°C, suitable for green synthesis due to selective antioxidant recovery and reduced toxicity [22].

2.3 Green Preparation of ZnO NPs

Zinc oxide nanoparticles were synthesized by mixing 20 mL of 0.1 N zinc acetate dihydrate with 20 mL of 25% aqueous methanol extract of Azadirachta indica knot wood in a 1:1 ratio. The mixture was stirred at 600 rpm for 3 hours, forming a golden-brown paste. After centrifugation and washing, the sample was oven-dried at 80 °C for 30 hours. The dried powder was annealed at 410 °C for 3 hours to improve crystallinity and remove organic residues. The ZnO NPs were then vacuum sealed and stored [23].

1.4 Characterization Methodologies

The morphology, composition, and resulting surface interactions of the nanocomposites were studied using scanning electron microscopy (SEM), X-ray photoelectron spectroscopy (XPS), and infrared (IR) spectroscopy.

The prepared ZnO NPs were primarily investigated by the X-ray diffraction (XRD) and SEM (Scanning Electron Microscopy). The crystalline structure and phase purity were determined by X-ray diffraction analysis using Bruker, D8 Advance ECO diffractometer with Cu-Kα radiation (λ = 1.5418 Å) at 40 kV and 30 mA. The surface topography and particle size were observed by a SEM Carl-Zeiss, Ultramicroscope 55, Germany. Particle size calculations The size of particles was estimated using the Debye– Scherrer equation from XRD data [24].

2.5 Evaluation of the Antifungal Activity

2.5.1 Preparation of Inoculum

For Laetiporus sulphureus and Pycnoporus sanguineus, a spore suspension was made by inoculating fungal cultures onto SDA plates followed by incubation for 5–7 days. The spores were collected with sterile distilled water and adjusted to a concentration of 1×10^6 spores/mL with a haemocytometer [25].

2.5.2 Well Diffusion Method

The antifungal potential of the green-produced ZnO NPs was assessed by agar well diffusion method. Filter-sterilized spores soruspension were inoculated onto SDA plates by swabbing. The agar was punctured with sterile cork borer of 6 mm in diameter, and then 50 µL of ZnO nanoparticles suspension (1 mg·mL−1 in sterile water) was introduced. The plates were then incubated at 28 ± 2°C for 48 h. Positive control used was fluconazole (20 µg/mL) while negative control was sterile distilled water [26].

2.5.3 Determination of Zone of Inhibition

The antifungal activity was then determined as the diameter (in mm) of clear zones around each well by digital Vernier caliper after incubation. Each assay was done in triplicate and the mean value at the nearest point of the standard deviation was reported [27].

2.5 Characterization of Samples

To fully visualize the morphology and characteristics of ZnO nanoparticles, various analytical facilities were applied. The functional groups and their chemical states were identified by FTIR. XRD apparatus was used to examine the crystal structure of the NPs, and SEM was employed to characterize and size the particle.

3. Results and Discussion

3.1 UV-Visible spectroscopy

The optical absorption spectra of the biosynthesized ZnO nanoparticles was studied by UV-Visible spectroscopy which showed excellent absorption peak at 368nm which is of quantum confinement effect compared to the bulk(377nm) ZnO. This particle size and synthetic condition dependent effect causes perturbation in electronic structure with an increase in bandgap. Optical band gap of 3.15 eV was determined from Tauc's plot which is in line with what has been reported for green synthesis of ZnO NPs. These results indicate the successful realization of ZnO NPs with nanoscale features and changed optical properties, which are attractive for high surface area and bandgap-tuning applications.

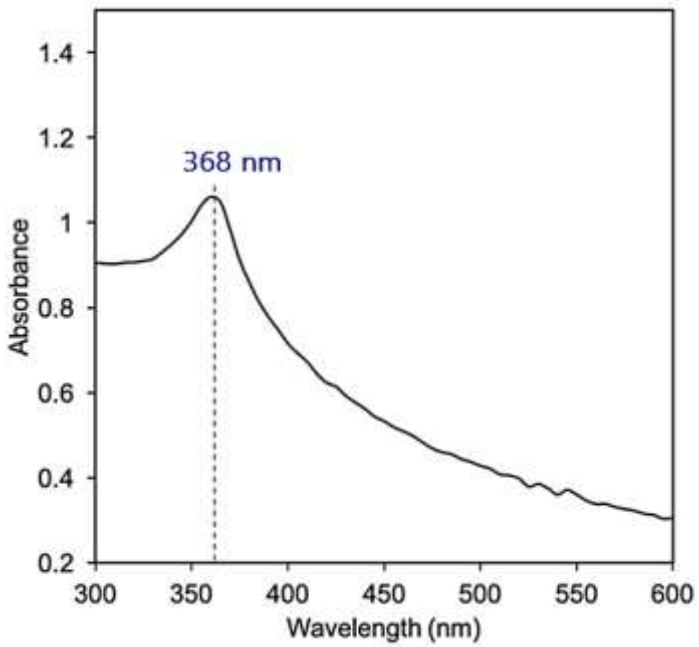

4.

Figure 1. UV-Visible Absorption Spectrum of biosynthesised ZnO NPs

3.2 FTIR Analysis

The FTIR spectra (Fig. 2 in the original paper) reveals some information regarding the chemical composition of the ZnO nanoparticles prepared using different amounts of knotwood extract. Key vibrational bands were thought to be observed in spectra recorded at room temperature in the region of 450–4500cm⁻¹.

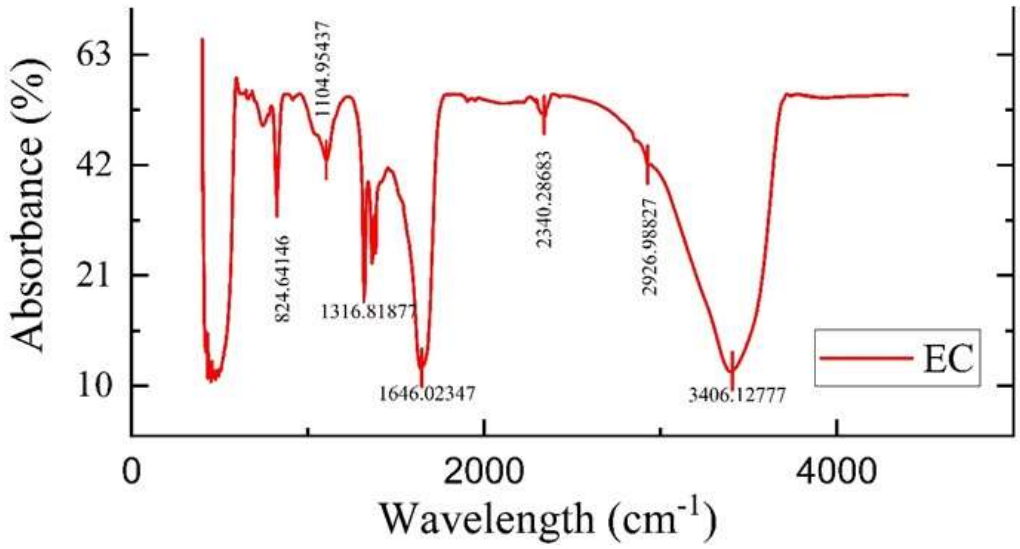

Figure 2: FTIR spectrum depicting ZnO synthesized from knot wood extract

A major peak 1645cm⁻¹ of the C=C stretching of aromatic ring and C=O stretching of polyphenols was observed. Another bands observed at 861cm⁻¹ is probably due to C–H bending in aromatic rings. Moreover, a sharp band at 1378cm⁻¹ indicates C–C stretching of aromatics that assist in NP formation.

Critically, all ZnO samples showed a sharp peak at ~618cm⁻¹ due to the Zn–O mode. This supports the formation of ZnO and is consistent with the previous results that the wavenumber is a characteristic peak fingerprint for zinc oxide nanoparticle [28].

3.3 XRD and Atomic Structure Properties

The XRD patterns (Fig. 3) showed more information regarding the crystalline structure of the ZnO NPs. Peaks were located at 2θ values of 31.78°, 34.44°, 36.28°, 47.55°, 56.62°, 62.83°, and 67.96° which could be described as the (100), (002), (101), (102), (110), (103), and (112) planes of hexagonal Wurtzite ZnO, according to the JCPDS card No. 36-1451 [23].

More importantly, these diffraction peaks were sharp and narrow, indicative of the synthesized samples being polycrystalline with no evidence of impurity crystalline phases or amorphous phase. This purity renders the green synthesized ZnO nanoparticles to be of similar quality as the ones prepared using conventional, mostly chemical means. The crystallite sizes were determined by Scherrer's equation [29]:

$$\tau = K\lambda / \beta\cos\theta$$

where τ is the crystallite size, K is the shape factor (usually 0.9), λ is the X-ray wavelength, β is the peak full width at half maximum in radian and θ is the Bragg's angle.

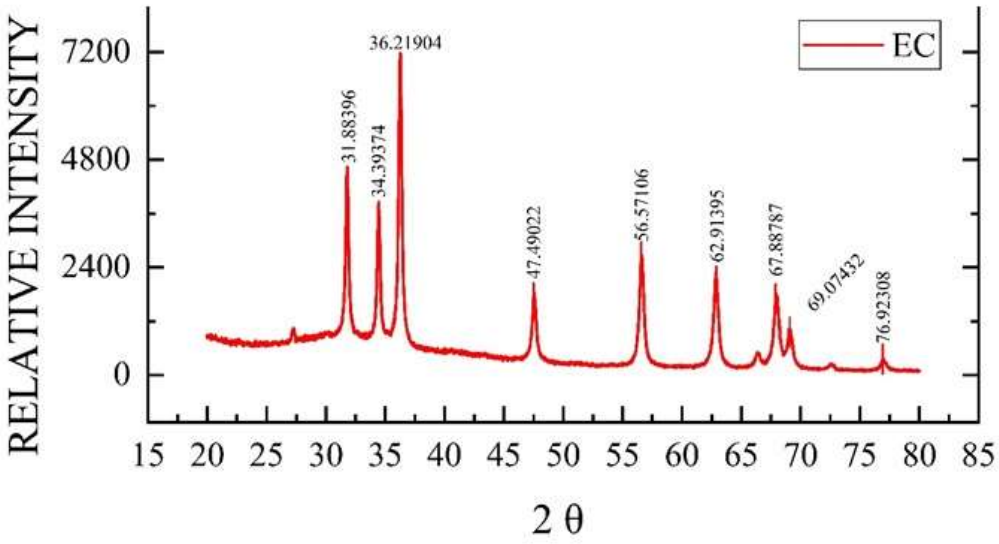

Figure 3: The XRD pattern of ZnO synthesized from knot wood

By using this formula, the average crystallite size of ZnO NPs for samples EC10, EC20, EC30, and EC40 were calculated to be 17.47 nm, 13.51 nm, 10.34 nm, and 9.04 nm, respectively. These results demonstrate unequivocally that with increased quantity of knootwood extract, smaller ZnO crystallites are formed, possibly due to the presence of a higher concentration of biologically active molecules in the extract that control nucleation and growth.

3.4 Morphological Analysis

The high-resolution SEM images (Fig. 4) provided insight into the morphology of the ZnO nanoparticles as a function of the extract volume. A trend can be observed: samples were prepared with more Knootwood extract, the more regular spherical minuscule in size were the particles.

Particles in Sample EC10, made with the least amount of extract, were somewhat nonuniform and less defined and were not of uniform size. On the other hand, sample EC40, which was prepared with the highest amount of extract volume, resulted in well-defined, nearly spherical nanoparticles with a narrow size range on average about 8±0.5nm—nearly matching with that determined by XRD for crystallite size.

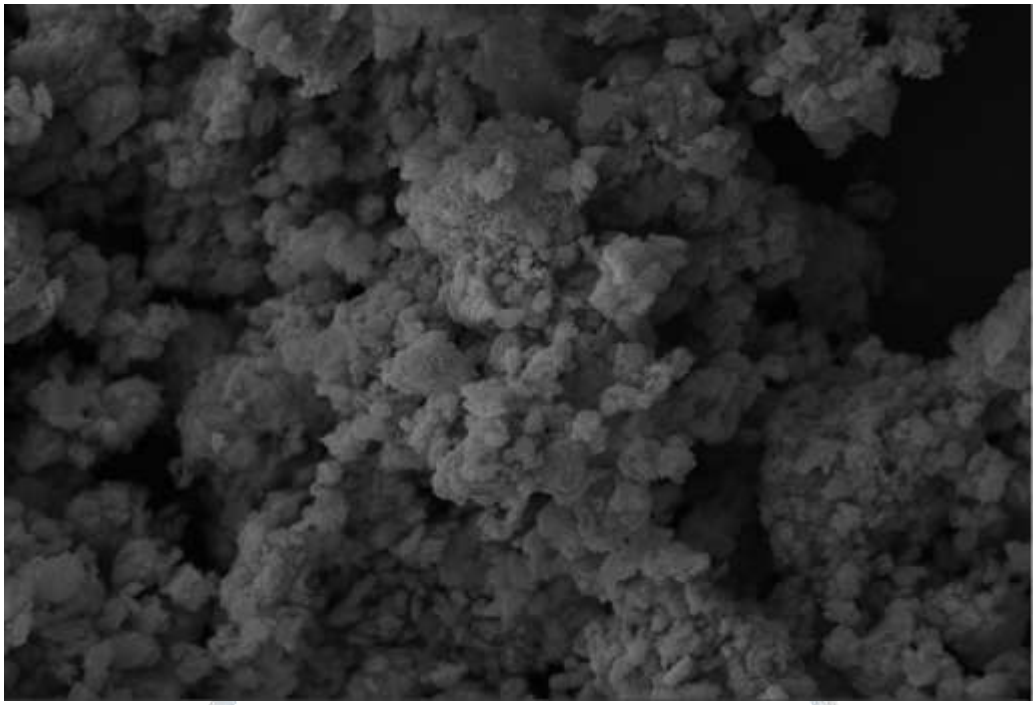

Figure 4: SEM images of synthesized ZnO NPs

This enhancement in morphology is due to polyphenolic compounds existing in knootwood extract influencing the rates of reduction and stabilizing the nanoparticles during the entire synthesis process [26]. Seems that the slow release of the zinc ions in contact to these phytochemicals was promoting a better control of size and structure homogeneity.

3.5 Antifungal activity

The antifungal potential of the green-synthesized ZnO nanoparticles was screened against L. sulphureus and P. sanguineus, two of the wood rot fungi highly recognized for their destructive roles on lignocellulosic biomass and wood composite materials. The inhibition was evaluated by the agar well diffusion method, and results are shown in Table 1.

Table 1. Antifungal potential of green-fabricated ZnO-nanoparticles

Fungal strain	**Zone of Inhibition (mm)**	**Positive Control (Fluconazole) (mm)**	**Negative Control (Water) (mm)**
Laetiporus sulphureus	19.2 ± 0.5	22.1 ± 0.3	0.0
Pycnoporus sanguineus	17.5 ± 0.6	20.6 ± 0.4	0.0

The ZnO-NPs showed highly antifungal effect against the tested fungi. More pronounced inhibitory zone was observed against Laetiporus sulphureus, pointing to better sensitivity to the nanoparticle treatment. This may be due to the interaction of nanoparticles with the fungal cell wall and the release of Zn^{2+} ions that disrupt metabolic pathways and generate oxidative stress by the formation of ROS [16], [17].

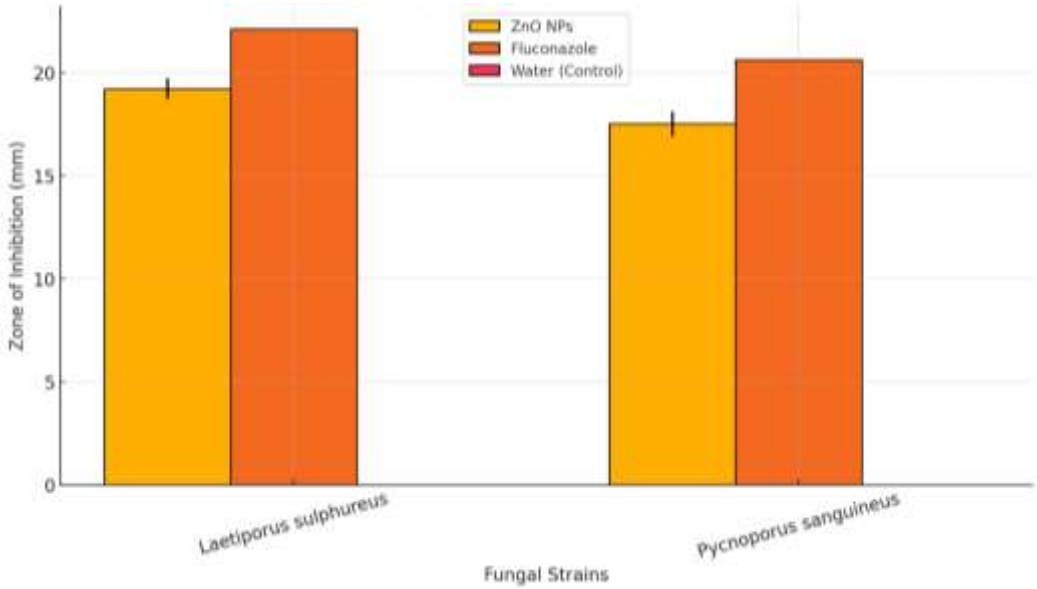

Figure 4: Antifungal activity of ZnO NPs

The results imply the prospective use of biogenic synthesized ZnO nanoparticles in defense of wood and plant based materials against basidiomycetous fungi associated with biodeterioration of wood and the applicability of eco-friendly wood preservation methods.

Conclusion

This research presents an uncomplicated, eco-compatible process for synthesizing ZnO nanoparticles and also compares the relative efficacy of aqueous extracts of Knootwood (knootwood) (as reducing and capping agent) for the above mentioned process. The size and monodispersity of the nanoparticles were adjusted by changing the quantity of extract in the synthesis. The pure-phase Wurtzite ZnO was successfully synthesised as confirmed by the structural characterization, and it was observed that the crystallite size of ZnO decreased with the increase in the extracted volume.

The one obtained with maximal amount of knootwood extract (EC40) presented the highest antifungal efficiency, degrading more than 84% of methylene blue in only 120 min. This performance is higher than that of the ZnO nanoparticles prepared by the regular chemical methods, that, in general, use toxic reagents and produced more waste.

In general, the green synthesis process presented in this study provides a sustainable, low-toxic method to prepare a high-performance ZnO nanoparticle which can use an environmental treatment application such as dye degradation.

References

[1] T. Robinson, G. McMullan, R. Marchant, P. Nigam, Remediation of dyes in textile effluent: a critical review on current treatment technologies with a proposed alternative, *Bioresource Technology*, 77 (2001) 247–262.

[2] Y.Z. Chen, N. Li, Y. Zhang, L.D. Zhang, Novel low-cost Fenton-like layered Fe-titanate catalyst: Preparation, characterization and application for degradation of organic colorants, *Journal of Colloid and Interface Science*, 422 (2014) 9–15.

[3] M. Shah, Effective treatment systems for azo dye degradation: A joint venture between physico-chemical & microbiological process, *International Journal of Environmental Bioremediation & Biodegradation*, 2 (2014) 231–242.

[4] D. Sudha, P. Sivakumar, Review on the photocatalytic activity of various composite catalysts, *Chemical Engineering and Processing: Process Intensification*, 97 (2015) 112–133.

[5] H.P. Suryawanshi, S.G. Bachhav, D.R. Patil, Hydrothermal synthesis of Zinc Oxide and its photocatalytic effect, *International Journal of Chemical and Physical Sciences*, 4 (2015) 483–486.

[6] J.C. Chen, C.T. Tang, Preparation and application of granular ZnO/Al_2O_3 catalyst for the removal of hazardous trichloroethylene, *Journal of Hazardous Materials*, 142 (2007) 88–96.

[7] I.K. Sen, K. Maity, S.S. Islam, Green synthesis of gold nanoparticles using a glucan of an edible mushroom and study of catalytic activity, *Carbohydrate Polymers*, 91 (2013) 518–528.

[8] M. Darroudi, Z. Sabouri, R.K. Oskuee, A.K. Zake, H. Kargar, M.H.N.A. Hamid, Sol–gel synthesis, characterization, and neurotoxicity effect of Zinc Oxide nanoparticles using gum tragacanth, *Ceramics International*, 39 (2013) 9195–9199.

[9] S. Chauhan, M.K. Upadhyay, N. Rishi, S. Rishi, Phytofabrication of silver nanoparticles using pomegranate fruit seeds, *International Journal of Nanomaterials and Biostructures*, 1 (2011) 17–21.

[10] K. Govindaraju, V. Kiruthiga, R. Manikandan, T. Ashokkumar, G. Singaravelu, β-glucosidase assisted biosynthesis of gold nanoparticles: A green chemistry approach, *Materials Letters*, 65 (2011) 256–259.

[11] D. Phillip, Honey mediated green synthesis of gold nanoparticles, *Spectrochimica Acta Part A: Molecular and Biomolecular Spectroscopy*, 73 (2009) 650–653.

[12] S.S. Shankar, A. Rai, A. Ahmad, M. Sastry, Rapid synthesis of Au, Ag, and bimetallic Au core–Ag shell nanoparticles using Neem (*Azadirachta indica*) leaf broth, *Journal of Colloid and Interface Science*, 275 (2004) 496–502.

[13] K.N. Thakkar, S.S. Mhatre, R.Y. Parikh, Biological synthesis of metallic nanoparticles, *Nanomedicine: Nanotechnology, Biology and Medicine*, 6 (2010) 257–262.

[14] K. Elumalai, S. Velmurugan, S. Ravi, V. Kathiravan, S. Ashokkumar, Green synthesis of zinc oxide nanoparticles using *Moringa oleifera* leaf extract and evaluation of its antimicrobial activity, *Spectrochimica Acta Part A: Molecular and Biomolecular Spectroscopy*, 143 (2015) 158–164.

[15] S. Iravani, Green synthesis of metal nanoparticles using plants, *Green Chemistry*, 13 (2011) 2638–2650.

[16] J.M. Lü, P.H. Lin, Q. Yao, C. Chen, Chemical and molecular mechanisms of antioxidants: experimental approaches and model systems, *Journal of Cellular and Molecular Medicine*, 14 (2009) 1582–4934.

[17] H. Muroi, I. Kubo, Combination effects of antibacterial compounds in knootwood flavor against *Streptococcus mutans*, *Journal of Agricultural and Food Chemistry*, 41 (1993) 1102–1105.

[18] A.R. Vilchis-Nestor, V. Sanchez-Mendieta, M.A. Camacho-Lopez, R.M. Gomes-Espinosa, M.A. Camacho-Lopez, J.A. Arenas-Alatorre, Solventless synthesis and optical properties of Au and Ag nanoparticles using *Knootwood* extract, *Materials Letters*, 62 (2008) 3103–3105.

[19] H. Çolak, E. Karakose, Green synthesis and characterization of nanostructured ZnO thin films using *Citrus aurantifolia* (lemon) peel extract by spin-coating method, *Journal of Alloys and Compounds*, 690 (2017) 658–662.

[20] S.R. Senthilkumar, T. Sivakumar, Knootwood (*Knootwood*) mediated synthesis of Zinc Oxide (ZnO) nanoparticles and studies on their antimicrobial activities, *International Journal of Pharmacy and Pharmaceutical Sciences*, 6 (2014) 461–465.

[21] R.K. Shah, F. Boruah, N. Parween, Synthesis and characterization of ZnO nanoparticles using leaf extract of *Knootwood* and evaluation of their antimicrobial efficacy, *International Journal of Current Microbiology and Applied Sciences*, 4 (2015) 444–450.

[22] R. Yuvakkumar, J. Suresh, B. Saravanakumar, A. Joseph Nathanael, S.I. Hong, V. Rajendran, Rambutan peels promoted biomimetic synthesis of bioinspired zinc oxide nanochains for biomedical applications, *Spectrochimica Acta Part A: Molecular and Biomolecular Spectroscopy*, 137 (2015) 250–258.

[23] C.Y. Yu, Y.R. Wang, Y. Liu, C.F. Guo, Y. Hu, Facile growth of ZnO nanocrystals on nitrogen-doped carbon nanotubes for visible-light photodegradation of dyes, *Materials Letters*, 100 (2013) 278–281.

[24] A. Kołodziejczak-Radzimska, T. Jesionowski, Zinc Oxide—From synthesis to application: A review, *Materials*, 7 (2014) 2833–2881.

[25] A.L. Patterson, The Scherrer formula for X-ray particle size determination, *Physical Review*, 56 (1939) 978–982.

[26] T.M. Rababah, N.S. Hettiarachchy, R. Horax, Total phenolics and antioxidant activities of fenugreek, knootwood, black tea, grape seed, ginger, rosemary, gotu kola, and ginkgo extracts, vitamin E, and tert-butylhydroquinone, *Journal of Agricultural and Food Chemistry*, 11 (2004) 5183–5189.

[27] S.H.S. Chan, T.Y. Wu, J.C. Juan, C.Y. Teh, Recent developments of metal oxide semiconductors as photocatalysts in advanced oxidation processes (AOPs) for treatment of dye wastewater, *Journal of Chemical Technology and Biotechnology*, 86 (2011) 1130–1158.

[28] K. Koci, L. Obalova, L. Matejova, D. Placha, Z. Lacny, J. Jirkovsky, O. Solcova, Effect of TiO_2 particle size on the photocatalytic reduction of CO_2, *Applied Catalysis B: Environmental*, 89 (2009) 494–502.

[29] T. Karnan, S.A.S. Selvakumar, Biosynthesis of ZnO nanoparticles using rambutan (*Nephelium lappaceum L.*) peel extract and their photocatalytic activity on methyl orange dye, *Journal of Molecular Structure*, 1125 (2016) 358–365.